Conservation of Isobaric Spin in the Reaction $Be^9(p,\alpha)Li^6$

R. MALM AND D. R. INGLIS
Argonne National Laboratory, Lemont, Illinois
(Received May 10, 1954)

The reaction $Be^9(p,\alpha)Li^6$ involves transitions to the ground state and first excited state of Li^6 which are shown to display only a gradual dependence on proton energy and no indication of resonance at the known gamma-ray resonance at 2.565 Mev which goes by way of the second excited state of Li^6. This may be explained in terms of conservation of isobaric spin and verifies that the second excited state of Li^6 has isobaric spin $T=1$ (or odd charge parity) as does also the resonant state of the compound nucleus B^{10}. The lack of resonance in the two alpha groups does not provide a very sensitive test of the purity of isobaric spin in the resonant state, because the contribution of an impurity would be superposed on a background, but the sharpness with which the gamma resonance falls off on the low-energy side does indicate that neighboring $T=0$ states have remarkably little $T=1$ admixture. The observations were made by means of a 16-in. two-dimensional focusing magnetic spectrometer, the construction and characteristics of which are described.

I. INTRODUCTION

THE reaction $Be^9(p,\alpha)Li^6$ yields relationships between some of the very light nuclei, the structure of which one would like to understand as completely as possible. Li^6 has been known[1] for over two years to have its lowest three states well separated from one another, the ground state with $J=1^+$. The first excited state at 2.187 Mev has recently been shown[2] to have $J=3^+$, as was expected theoretically,[3] and the second excited state at 3.58 Mev has been identified with the ground state of He^6, having thus $J=0^+$ and presumably isobaric spin $T=1$, as is also compatible with theoretical expectations. The experimental verification that this state has $T=1$ appeared in the early stages of this work[4] and is found very clearly in recent work[2,5] on deuteron scattering in helium.

Our investigation of $Be^9(p,\alpha)Li^6$ was started in the summer of 1951, when only one excited state of Li^6 had been recognized[6] because the gamma-ray energy[7] had not been measured carefully enough to show up a discrepancy, and our first indication that there must be two excited states came from the failure of the excited-state alpha group to display the gamma-ray resonance. The work suffered an unusually long delay while the laboratory was moved to a new site, and the spectrometer was considerably improved. The present interest of the results is mainly in their relation to the purity of isobaric spin.

II. EXPERIMENTAL APPARATUS

For the purposes of this investigation and other research relating to the properties of light nuclei, a high-resolution, two-dimensional focusing, magnetic spectrometer was constructed for use with the ANL statitron which provides monoergic protons or deuterons up to about $3\frac{1}{2}$ Mev. This spectrometer is designed to focus protons of energy up to 15 Mev and to be capable of admitting through a solid angle of approximately 0.01 steradian the products from nuclear reactions emitted at angles from zero to 135 degrees with respect to the bombarding particles. Since only a portion of the running time of the statitron is available for charged-particle research, the mounting of the spectrometer and the necessary electrical, water, and vacuum connections are designed to enable the spectrometer to be moved easily to and from the experimental area by use of an overhead crane.

The magnet is of an inhomogeneous field type explored by Siegbahn and is essentially the same as the magnet of the 16-in. proton spectrometer at the California Institute of Technology.[8] It differs from that one in having windings with internally cooled conductor and consequent high currents, and in some of the detailed dimensions. The cross section of the magnet is shown in Fig. 1. The pole pieces are shaped, as shown in Sec. A-A of Fig. 1, to provide a magnetic field with a radial dependence proportional to $r^{-\frac{1}{2}}$ in the midplane. The magnet is semicircular with a mean radius of 16 in. The dimensions of the gap are roughly 6 in. radially by 2 in. in depth, providing the possibility of a fairly large solid angle in which the particles may emerge from a point in the target and still be focused to a point (aside from slight astigmatism) in the focal plane.

The magnet windings consist of 20 kidney-shaped coils, each coil consisting of 7 turns of $\frac{3}{8}$-in. square copper bar having a $\frac{1}{8}$-in. square hole for cooling purposes. The twenty kidney-shaped coils fit snugly around the poles as shown in Fig. 1. The coils are connected in series, and power is supplied by a 600-amp, 40-v welding

[1] F. Ajzenburg and T. Lauritsen, Revs. Modern Phys. **24**, 321 (1952).
[2] Lauritsen, Huus, and Nilsson, Phys. Rev. **92**, 1501 (1953).
[3] D. R. Inglis, Revs. Modern Phys. **25**, 390 (1953).
[4] Reference 1, p. 347.
[5] H. T. Richards and A. Galonsky (private communications).
[6] Hornyak, Lauritsen, Morrison, and Fowler, Revs. Modern Phys. **22**, 219 (1950).
[7] R. B. Day and R. L. Walker, Phys. Rev. **85**, 582 (1952).
[8] Svartholm and Siegbahn, Arkiv Mat. Astron. Fysik **A33**, Nos. 21, 24 (1946); Snyder, Rubin, Fowler, and Lauritsen, Rev. Sci. Instr. **21**, 852 (1950); W. Whaling and C. W. Li, Phys. Rev. **81**, 150 (1951). C. Mileikowsky, Arkiv Fysik **4**, 337 (1952); **7**, 33, 47 (1954).

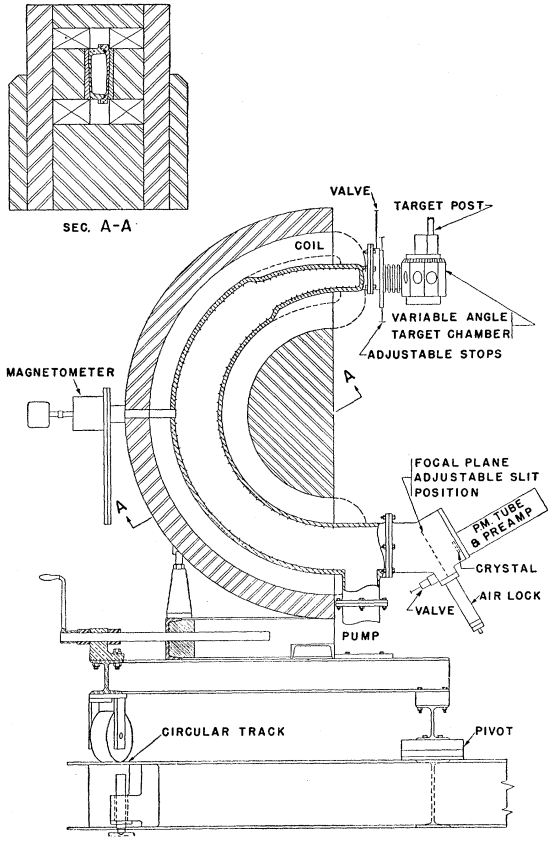

FIG. 1. The two-dimensional-focusing "proton spectrometer."

generator. The windings are cooled internally by the flow of distilled water in a closed system consisting of the windings, turbine pump, heat exchanger, and reservoir. To prevent condensation of moisture in the windings, the heat exchanger is automatically by-passed when the water temperature drops below a certain temperature.

The magnet is supported on four jacks which rest on a pivoted stand. This stand travels on a circular track and permits variations in the angular position through about 135°, permitting observation of angular distributions of the product particles of nuclear reactions.

To articulate the vacuum system and permit this observation at various angles in a horizontal plane with a horizontal incident beam, a variable-angle target chamber is used. It consists essentially of two parts with matching cylindrical surfaces. The fixed inner part contains a fixed beam entrance aperture, an adjustable post holding the target along the vertical central axis, and a wide horizontal exit slot permitting egress at all angles between about 140° from the beam direction and 0° or a little beyond. The exit slot is surrounded by an O-ring groove in the outer cylindrical surface and covered by the inner cylindrical surface of the sliding outer part of the target chamber. The continuous sliding motion about the vertical axis is limited to an angle of about 30° because of the conflict with the beam entrance in the backward direction, so the outer part of the chamber contains several exit ports spaced at about 30°, making it possible to reach any angle within the range covered by the exit slot. The exclusion of angles more nearly backward than this arises from the thickness of the magnet (16 in.) and the limited "object distance" of the magnetic lens (11 in.). The target chamber also contains a vacuum valve wide enough to span the exit slot, making it possible to change ports without exposing the target to the atmosphere.

The particles leaving the target chamber pass through a sylphon bellows and enter the deflection chamber of the spectrometer through a variable aperture and a vacuum valve. Because of an excess downward deflection in the fringing field, the target chamber is mounted a little low, with the target spot about 8 mm below the horizontal extension of the median circle. The deflection chamber fits between the poles of the magnet as shown in Fig. 1. It consists of two aluminum castings, a boxlike structure, and a cover. The joint between them is sealed by means of a round gasket in a groove. In order to minimize scattering from the inner walls of the chamber, these walls are cast with narrow ridges about $\frac{1}{16}$ in. high and $\frac{3}{4}$ in. apart.

On leaving the lower end of the deflection chamber, the particles enter the detection chamber where particles of different monoenergetic groups are focused at various points along the focal plane indicated in Fig. 1. An air lock permits placing a photographic plate in this focal plane without breaking vacuum, but in the principal use of the instrument with electronic detection a defining slit of variable width is placed in this plane at the central position. Behind this, exposed directly to the vacuum, is a thin NaI(Tl) scintillation detector, kindly supplied by Mr. Robert Swank. Behind this is a 5819 photomultiplier feeding pulses into a 10-channel kicksorter. (A proportional counter was used for the earlier part of the work.) On the bottom of the detection

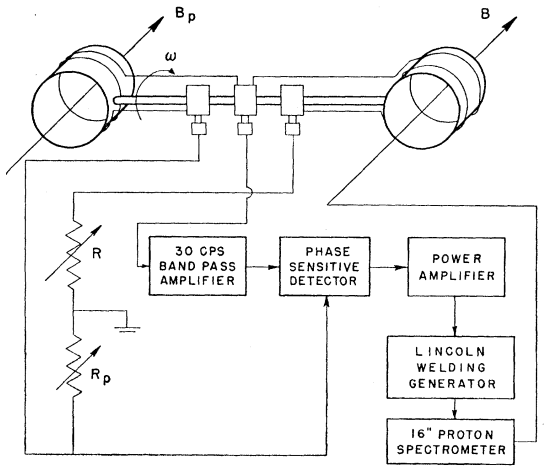

FIG. 2. Schematic diagram of the spectrometer magnet control.

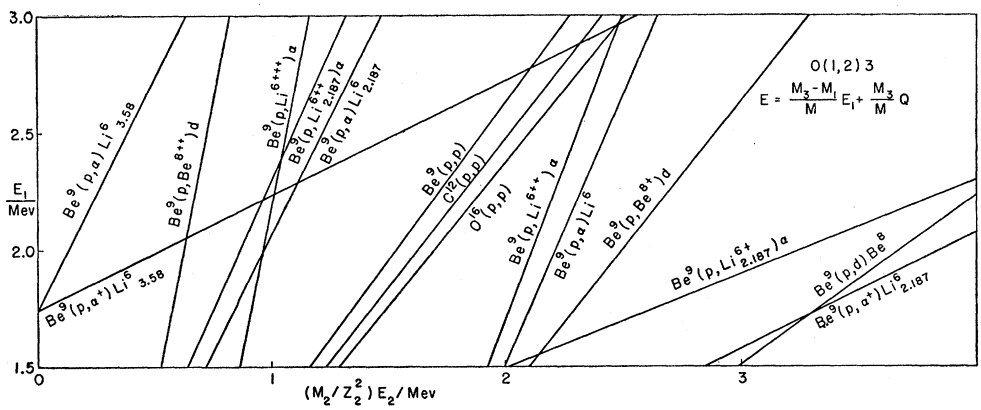

FIG. 3. Focusing field as dependent on bombarding energy for various ions.

chamber is a pumping port supporting a D.P.I. VFM260 diffusion pump.

The control and stabilization of the magnetic field is accomplished by means of the feedback system shown in Fig. 2. The sensing element is a rotating type magnetometer which generates two 30-cycle voltages, one proportional to the field of an Alnico V permanent magnet, the other proportional to the magnetic field in the central plane near the edge of the pole pieces of the spectrometer magnet. These voltages are added in phase and applied across the two 100 000-ohm resistance boxes. A signal is obtained from the network as shown in the diagram, passed through a 30-cycle band-pass amplifier and phase-sensitive detector, and the resulting dc signal is applied to the grids of three 807 cathode followers connected in parallel which drive the field windings of the exciter for the welding generator. The current supplied to the magnet tends to assume a value for which the input signal to the 30-cycle amplifier is zero. The field B thus obtained is related to the field B_p of the permanent magnet $B=B_pR/R_p$, and if B_p and R_p remain constant, B is proportional to R. Thus, adjusting R automatically produces a field in the spectrometer proportional to R.

This type of generating magnetometer has the advantage of ruggedness and the disadvantage that it measures the field only between the edges of the poles, since making its armature protrude any farther would intercept some of the valuable solid angle. The torsion type used by Lauritsen[9] can be made to present a very small area to the deflected particles when placed in the central position, but a modification of it employing quartz fibers to avoid fiber hysteresis was found to break as a result of fiber fatigue. The generating magnetometer has displayed a gradual drift on warming up of about 1 percent because of an unexpectedly large change of the permanent magnet field with temperature. This has been corrected since the measurements here reported were made by redesigning the magnetometer for use with a thermostated oil bath. At the fields employed in the work with magnet currents up to about 400 amp, fields to 10 kilo-oersteds, and deflected proton energies to 10 Mev, the focused particle momentum has been found to be proportional to the field observed at the edge to within the accuracy of observation permitted by the temperature variations. At higher fields, more serious nonlinearity from differential saturation may be anticipated.

[9] C. C. Lauritsen and T. Lauritsen, Rev. Sci. Instr. **19**, 916 (1948).

PULSE-HEIGHT DISCRIMINATION

With a given target and type of bombarding particle, the counting rate depends on the four variables bombarding energy E_1, magnet setting B, and two variables of pulse-height discrimination, say the channel width and channel level. When measuring a particle-energy spectrum with E_1 fixed and B variable, the range of pulse height must be chosen to give all or a representative sample of the pulses from particles of the desired sort. The 10-channel kicksorter helps greatly in eliminating trouble from these additional variables. It is ordinarily set so the peak in pulse size covers some of the middle channels with low counting rates in the end channels, which provides assurance that the total count is valid and indicates when an occasional change of channel level is needed.

At a given B it was found possible to distinguish by peak bias between Li^{++} ions, alphas, and protons (in ascending order of peak bias), but not to resolve these peaks completely, with the NaI crystal used in this work.

ENERGY DISTRIBUTION OF PRODUCT PARTICLES

A fairly thin (roughly 3×10^{-5} cm) beryllium target, of a type prepared by Dr. Hugh Bradner (and kindly supplied by him) by evaporation without adhesion onto a flexible steel backing from which it was peeled, cemented without backing in a light frame, was bombarded by protons of well-defined energy. The particles leaving the target are alphas, deuterons, Li^6 and Be^8 ions of various charges, as well as (elastically) scattered

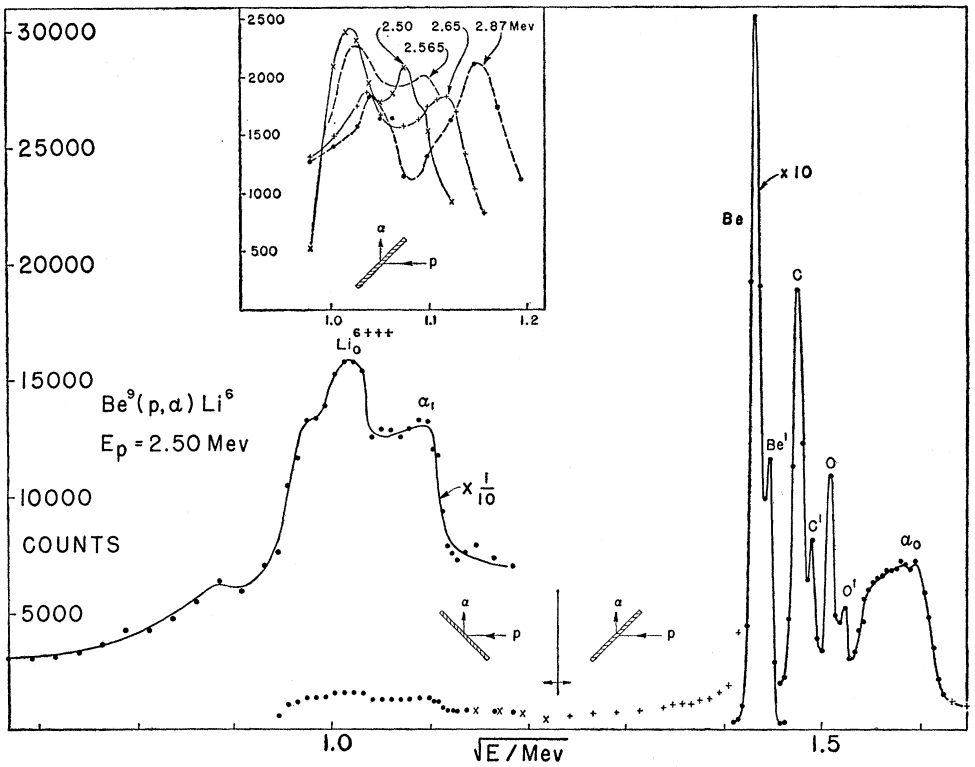

FIG. 4. The observed spectrum from a fairly thin Be target bombarded by 2.5-Mev protons.

protons. The (constant) radius of the median circle multiplied by the magnetic field B on it is proportional to the particle momentum divided by its charge, so B^2 is proportional to the energy E_2 of the product (of mass M_2 and charge Z_2e) through the quantity M_2E_2/Z_2^2. The dependence of this quantity on the incident proton energy E_1 for the various reactions, reaction energies, and product particles encountered is plotted in Fig. 3. This is based on data found in the literature[1] for reaction energies and for excitation energies of the various excited states of the final nuclei (indicated by subscripts, in Mev). Crossovers of these lines are places where particles of different energies and charges and/or masses are observed at the same magnetic field.

The appearance of the energy spectrum of the product particles observed at an incident proton energy $E_p=E_1=2.50$ Mev is shown in Fig. 4. The abscissa gives energy directly in Mev for alphas and protons, $(3/2)^{\frac{1}{2}}E_2$ for the Li^{6++} ions that happen to fall near the alpha groups. The main reaction peak corresponding to the ground state of Li^6 is seen at the right, near 1.6 Mev, and the much weaker peak corresponding to the 2.187-Mev excited state appears in the vicinity of 1 Mev. The ordinate gives number of counts per observed point but the numbers for the weak peak have been multiplied by ten in plotting the secondary curve that shows the shape of the peak. Both these peaks are quite broad as a result of target thickness, and in neither of them is the alpha peak resolved from the Li-ion peak. The sharp elastic-scattering peaks from the Be target and from C and O impurities (surface layers) are to be seen near 1.5 Mev, together with their "ghosts" which are discussed below.

Target orientation as well as target thickness, of course, influences the shape of the peaks observed, and two orientations were used in the observations of Fig. 4, as indicated by the small inserts. The "transmission" orientation indicated at the lower right and used above about 1.2 Mev tends to give sharper peaks than does the "reflection" position at the left, since even at 45° the transmission orientation more nearly approximates the ideal orientation nearer grazing incidence in which the energy loss by a proton traversing the foil to make a reaction on the back surface is the same as that of an alpha traversing it from a reaction on the front surface. The excited-state peak is broader not only because the "reflection" orientation was used but also because of the greater specific energy loss of the lower-energy emerging particles. It will be noted, too, that in Fig. 3 there is a juxtaposition of three possible energy groups in this region, and the peak at 1.0 Mev rising above the broader plateau is attributed to Li^{6+++} ions from the ground-state transition. This identification was possible as a result of the subsidiary observations depicted in the insert at the top of Fig. 4. Here the "transmission" orientation was used for better resolution, and the bombarding energy E_p was varied, displaying the property that the position of the Li-ion

ground-state group is less sensitive to bombarding energy (showing a steeper rise in Fig. 3). The observed energy dependence of the peak shape makes it appear that the Li^{6++} excited state group is relatively weak. It would be expected to be a little broader than the other two.

THE SPECTROSCOPIC "GHOSTS"

It is interesting to observe in Fig. 4 that this heavy-particle spectroscopy has something more than a name in common with the early days of optical spectroscopy in the appearance of "ghosts." The elastic scattering peaks are much sharper than the others because they do not involve the egress of a highly ionizing particle heavier than a proton from the target, and each of them displays a satellite peak of slightly higher apparent momentum, giving the composite peak a rather similar structure in all three cases. If it appeared only for C and O, one might want to attribute it to surface layers on the front and back of the target, but its appearance (marked Be′) on the side of the Be peak too makes it clear that it must be instrumental.

The ghosts appear to arise from secondary scattering from the small-radius side of the deflection chamber, for they could be eliminated by reducing the entrance aperture from its lower side. Particles entering the surface at nearly grazing incidence can by relatively intense small-angle scattering emerge with slightly reduced energy, and the outward change in direction may be just compensated by the greater inward magnetic deflection over the remainder of the path as a result of the energy loss, permitting the particle to reach the exit slit. The emerging energy may decrease with increasing angle in a fairly definite way, giving a focusing effect in the neighborhood of an optimum scattering angle. It seems plausible that a focus caused by balancing the effects of energy loss and scattering angle might fall near the focus where the particle would have arrived without scattering if the chamber had been wider.

EXCITATION CURVES

The intensities of various reaction products of interest were observed as functions of bombarding energy, with particular emphasis on the immediate neighborhood of $E_p = 2.565$ Mev where the 3.6-Mev gamma ray resulting from the transition to the second excited state of Li^6 shows a pronounced resonance. (This resonance was, in fact, used to calibrate our energy scale, because a new 90° electrostatic deflector on the diatomic beam was used to control the statitron for the first time during this work.) These data are shown in Fig. 5, on the left on a contracted scale to cover a broad energy region and on the right on an expanded scale to cover the resonance region. The points marked α_1 and indicated as dots show the behavior of the shoulder near 1.1 Mev of the low-energy peak in Fig. 4. It passes smoothly through the resonance region with no fluctuations outside of statistical expectations, and starts to rise slightly at lower energies. In following it to lower energies, as suggested by extrapolating from the trend in the insert of Fig. 4, the shoulder merges with the Li^{6+++} ground-state peak and from there on to lower energies that peak was followed as the alpha peak "passed under it," the resultant intensity being shown by the crosses marked $\alpha_1 + Li_0^{6+++}$ in Fig. 5. The curve shows only a very gradual rise and fall, with no pronounced resonance structure at all. Readings were taken at 20-kev intervals, and over some short regions at intervals as small as 8 kev in an unsuccessful attempt to resolve any fine structure there might be. As a result of this lack of structure, the data taken for the other particle groups are more sketchy, but also show no evidence for anything but a fairly gradual change of intensity with energy. The ground-state alphas, indicated by circles,

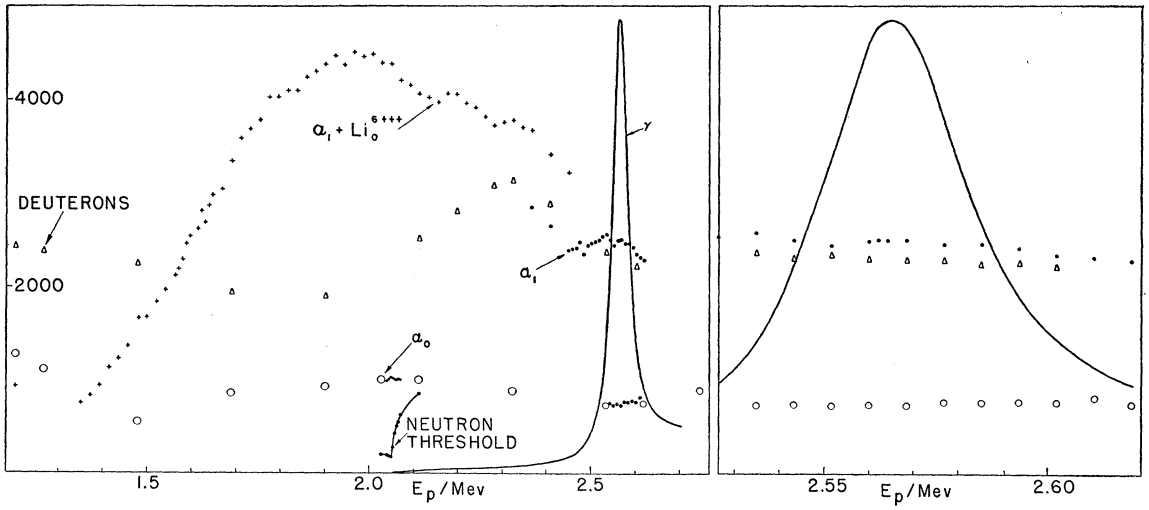

FIG. 5. Excitation curves for the various energy groups of the heavy-particle spectrum and for the 3.58-Mev gammas.

show an initial decrease between 1.2 and 1.5 Mev, indicating how the curve joins on to the low-energy curve reported earlier.[10] The curve then shows a much more gradual rise from 1.5 to 2 Mev than does the α_1+Li_0^{6+++} curve, indicating that the rise must arise largely from the composite nature of the latter. The maximum does indeed agree closely with the crossover of the curves labeled $Be^9(p,\alpha)Li^6_{2.187}$ and $Be^9(p,Li^{6+++})\alpha$ in Fig. 3. The ground-state alphas are seen to pass very smoothly past the gamma resonance and to show no influence of neutron competition at the $Be^9(p,n)$ threshold, the observation of which with a "long counter" is indicated at 2.06 Mev. The deuterons from $Be^9(p,d)Be_0^8$, indicated by deltas, show a fairly pronounced maximum (not entirely expected for a stripping reaction) at 2.3 Mev, and pass smoothly (as in this case is hardly surprising) through the γ-resonance region as shown in the right side of Fig. 5.

The width at half-maximum of the gamma resonance plotted in Fig. 5 is 43±1 kev. From the low-energy tail extending down to the neutron threshold, it is apparent that there is some neutron background, and if a background linearly interpolated between the apparent backgrounds on the two sides of the resonance is subtracted off, the width at half-maximum is reduced to 41±2 kev, in agreement with the reported value[10] 39±2 kev.

CONCLUSIONS

The fact that none of the excitation curves observed seems to show any sharp or pronounced resonances, no more than a gradual rise and fall, in the region 1.3 to 2.7 Mev suggests that the level density in this region of excitation of the compound nucleus, 7.7 to 9 Mev in B^{10}, is too high in comparison with the level width for the levels to appear individually. This is consistent with what is known of the energy levels just below this region,[1] where they are dense and expected to continue to increase in density at higher energies, and with the known behavior[10] of the ground-state alpha curve below 1.1 Mev.

The most striking feature of these results is the completeness with which the α_0 and α_1 curves exclude any appearance of resonance as they pass through the gamma resonance. The explanation has already been suggested on the basis of a preliminary report of these results[4] and involves the conservation of isobaric spin. The second excited state of Li^6 at 3.58 Mev is known to have isobaric spin $T=1$ both from the agreement with the energy of the ground state of He^6, after application of the Coulomb correction, and more recently from the failure of the deuteron scattering on helium to show any resonant behavior at this energy level.[5] One has then but to assume that the resonant level at $E_p=2.565$ Mev, or at an excitation energy 8.89 Mev in the compound nucleus B^{10}, is a $T=1$ level to understand the selective transition to the $T=1$ but not to the $T=0$ levels of $Li^6+\alpha$, or rather of Li^6 since the alpha has $T=0$. (If one wishes to make the distinction between charge symmetry and charge independence of nuclear forces, the same statements may be made less restrictively by replacing $T=1$ and 0 by charge parity odd and even, except for the statement about the level of He^6.) The low states of Li^6 are a particularly favorable place for the expectation of high purity of isobaric spin, the Coulomb energy being so small and the levels widely spaced. B^{10} is also favorable in having small Coulomb energy, but the $T=1$ value seems to be confined quite completely to the 8.89 level in spite of the high density of $T=0$ levels nearby.

The failure of the α_0 and α_1 curves to show any resonance behavior at 2.565 Mev is not a very sensitive test of the purity of the isobaric spin $T=1$, without any $T=0$ admixture, of the compound state at that level, because the effect of a small $T=0$ admixture would be superposed on the background provided by essentially a continuum of $T=0$ states.

The most convincing evidence of lack of isobaric spin mixing is the rather sharp tailing off of the gamma resonance toward low energies, indicating that the $T=0$ states of B^{10} just below the resonance are quite pure, not much contaminated by $T=1$ admixture from the 8.89-Mev state. Some of them would be expected to have the same J as this state. Since the "tail" starts at the neutron threshold, a considerable part of it may be attributed, in spite of its proximity, to neutrons, but how much was unfortunately not ascertained. Thus the height of the "tail" indicates only an upper limit to the amount of $T=1$ admixture.

The $T=0$ level of Li^6 at 2.187 Mev does not give a gamma because its isobaric spin $T=0$ (as well as its $J\neq 0^+$) permits it to disintegrate into an alpha and a deuteron, an essentially faster process. The fact that the gamma results only from a $T=1$ level of the compound nucleus explains in a general way why we should observe a pronounced gamma resonance against a continuous background of the other transitions arising from essentially a continuum of levels at high-excitation energies where a high density of $T=0$ levels, but not of $T=1$ levels, may be expected. The density of $T=1$ levels is, however, not so very low: there is one in Be^{10} at the B^{10} equivalent of 8.0 Mev, which is just too low to go to the 3.58-Mev state of Li^6; and there are two close together just above 8.89 Mev, one (assigned[11] 3^+) at 9.12 Mev and the other (>0) at 9.24 Mev. It is thus not clear that there should be only one gamma resonance in this region, until one takes into account the low energy available for the alpha going to the 3.58-Mev

[10] Hahn, Snyder, Willard, Blair, Klema, Kingston, and Green, Phys. Rev. **85**, 934 (1952).

[11] Adair, Barshall, Bockelman, and Sala, Phys. Rev. **75**, 1124 (1949).

state which would be expected to bring angular momentum selection rules into play. If the B^{10} state at 8.89 Mev corresponds to the Be^{10} state at the equivalent of 9.24 Mev with, say, $J=1$ or 2, it could make the transition with $l_\alpha=0$ or 1 much more easily than could a B^{10} state with $J=3^+$, requiring $l_\alpha=2$. Thus the 3^+ assignment to one of the two Be^{10} states helps to explain why the gamma resonance is not double.

In summary, the appearance of a single gamma resonance where the higher-energy alphas show only the influence of a continuum of states may indeed be explained by assuming conservation of isobaric spin.

ACKNOWLEDGMENTS

We are grateful to C. C. Lauritsen and W. Whaling of the California Institute of Technology for early design and performance information on their spectrometer, to G. M. Lobell, R. K. Swank, T. Brill, and J. P. McMahon for help with the construction and electronics of our spectrometer, to A. S. Langsdorf, Jr., R. E. Holland, F. P. Mooring, J. R. Wallace, and R. R. Weeks for their contributions to the performance of the statitron and its appurtenances, to H. Bradner of Berkeley for thin Be targets, and to L. Darlington for participation in taking the data.

PHYSICAL REVIEW VOLUME 95, NUMBER 4 AUGUST 15, 1954

Decay of the Odd-Odd Isomer Tl^{198m}†

T. O. PASSELL, M. C. MICHEL, AND I. BERGSTRÖM*
Radiation Laboratory and Department of Chemistry, University of California, Berkeley, California
(Received May 4, 1954)

The electron spectrum of Tl^{198m} has been investigated in a 25-cm double-focusing beta spectrometer with a resolution of approximately 0.4 percent. The electron lines have been assigned to three gamma rays with energies (in kev) 261.5, 284, and 48.4, respectively. The multipolarities assigned from conversion ratio and lifetime considerations are $M4$, $M1+E2$, and $E2$, respectively. A tentative decay scheme is proposed which is consistent with all the available data.

I. INTRODUCTION

A 1.9-HOUR isotope of thallium was first observed and assigned to Tl^{198} by Orth *et al.*[1] Recently this activity has been independently assigned by two different groups of investigators to the decay of an isomeric state. The previously unobserved ground-state decays by electron capture to Hg^{198} with a half-life of 5.3 ± 0.5 hours.

Michel and Templeton[2] of this laboratory produced these activities by the $Au^{197}(\alpha,3n)Tl^{198}$ reaction in the Crocker Laboratory 60-inch cyclotron. Mass separation was made on a time-of-flight isotope separator[3] and the 1.75-hour and 5.3-hour activities shown to be Tl^{198}. Bergström, Hill, and DePasquali[4] at the University of Illinois produced the same activities by bombarding mercury with 11.5-Mev deuterons. Among the many electron lines they observed were several approximately 1.9-hour lines assignable to two gamma rays converting in thallium with energies of 282.4 and 260.7 kev, and a third gamma ray of 48.7 kev whose assignment was not unambiguous. The authors suggested that all three gamma rays were in cascade from an isomeric state having the unusually high spin of 9 with odd parity. Because of the unusual decay scheme suggested, the ambiguity of the 48.7-kev gamma-ray's assignment, and the uncertainties in the photographically determined intensities, further work on this isomer was thought to be desirable.

II. EXPERIMENTAL WORK

Means of Production and Chemical Separation

In this investigation 0.001-inch gold foil was bombarded in the Crocker Laboratory 60-inch cyclotron with 38-Mev helium ions to produce the Tl^{198m} by the $(\alpha,3n)$ reaction. This choice of foil thickness and bombarding energy was effective in minimizing the production of Tl^{199}.

The thallium was chemically separated from the gold target by the following process: (1) the gold was dissolved in aqua regia leaving the gold and thallium in solution as Au^{+3} and Tl^{+3} ions, respectively; (2) sulfur dioxide gas was bubbled through the solution to reduce the Tl^{+3} to Tl^+ and the gold to the metal; (3) the solution was centrifuged and supernatant containing Tl^+ and traces of Au^{+3} carried through varying purification procedures including an ethyl ether extraction; (4) the solution containing thallium was then passed through a Dowex A-2 ion exchange column in $6M$

† This work was performed under the auspices of the U. S. Atomic Energy Commission.
* On leave of absence from the Nobel Institute for Physics, Stockholm, Sweden, with a grant from Svenska Atomkommitten.
[1] Orth, Marquez, Heiman, and Templeton, Phys. Rev. **75**, 1100 (1949).
[2] M. C. Michel and D. H. Templeton, Phys. Rev. **93**, 1422 (1954).
[3] M. C. Michel, Ph.D. thesis, University of California Unclassified Report UCRL-2267, 1953 (unpublished).
[4] Bergström, Hill, and DePasquali, Phys. Rev. **92**, 918 (1953).